three-photon absorption by the neutral parent to the ^2E_u state of the ion would be in excess of the appearance potential of $C_4H_4^+$ but not that of the $C_4H_3^+$ ion. However, absorption of an additional 532-nm photon from the three UV photon level would promote the ion to an energy level well in excess of the appearance potential of the $C_4H_3^+$ daughter ion. Such an absorption depletes the population of the vibronic state of the parent ion at 14.0 eV (above the ground state of the neutral), the source of the $C_4H_4^+$ ions. This is manifested by a decrease in the amount of $C_4H_4^+$ daughter fragment observed. In other words, the secondary pump beam results in the formation of $C_4H_3^+$ at the expense of $C_4H_4^+$. With increasing delays, the falloff of the $C_4H_3^+$ ion current is similar to the increase observed for $C_4H_4^+$ ion current, supporting the proposal of the intermediacy of the vibronic state of the parent ion at 14.0 eV above the ground state of the neutral molecule.

Behavior of the $C_6H_5^+$ Mass Peak. Based on the appearance potentials of $C_4H_4^+$ and $C_6H_5^+$,[4,5] shown in Figure 1, one might expect that both ions would be formed via similar redistribution processes. However, unlike the dynamic behavior of $C_4H_4^+$, the $C_6H_5^+$ ion current as a function of delay between the two laser pulses, clearly reveals biexponential behavior at the higher UV laser powers. This is shown in Figure 3. At zero delay, the $C_6H_5^+$ ion current undergoes a decrease similar to that observed for $C_4H_4^+$. However, for $C_6H_5^+$ we observe recovery times on the picosecond as well as the nanosecond time scales. If we fit the fast component of the $C_6H_5^+$ curve to a single exponential, a half-life of 350 ± 100 ps is obtained. The nanosecond component appears to be, within experimental error, similar to that observed in the case of $C_4H_4^+$,[1] i.e., 20 ± 5 ns which is comparable to the observed lifetime of the $^2E_1$ state of the parent ion.[6] Figure 3 shows the results of the UV power dependence on the relative amplitudes of the picosecond and nanosecond components of the $C_6H_5^+$ daughter.

These results reveal that the rapid component becomes more pronounced at high UV power. These results can be explained as follows. The similarity between the recovery times of the $C_6H_5^+$ and $C_4H_4^+$ ions on the nanosecond time scale indicates that a common redistribution process leads to the formation of these daughter ions. This represents the energy redistribution of the vibronic level of the parent ion resulting from the absorption of three UV laser photons by the parent molecule. The observed power dependence on the relative amplitudes of the picosecond and nanosecond recovery times of $C_6H_5^+$ suggests that, in addition to the ^2E_u state, a higher electronic state of the parent ion (probably resulting from the absorption of an additional UV photon) gives rise to a species with a mass to charge ratio of 77. If one assumes that the UV laser power is not sufficiently high to produce doubly charged ion, this species could either be an excited state of the $C_6H_5^+$ formed from these UV photons or a higher energy isomer. One might also consider the possibility that the same $C_6H_5^+$ ion is formed from both states but, at high UV power, a neutral fragment in an excited state is formed. This can be ruled out in this particular case as the first excited state of the neutral fragment (atomic hydrogen) is about 10 eV higher than the ground state.

The Mechanism of MPID. A number of observations suggest that the formation of all the ions studied here results directly from the fragmentation of the parent ion, thus supporting an ionic ladder mechanism. We are able to successfully describe all of our dynamic and power dependence observations in terms of the ionic energy level diagram, the known lifetime of the lowest excited state state of the parent ion, and the appearance potential of these three ions.

The interrelation between the dynamics of formation of $C_4H_4^+$ and $C_4H_3^+$ gives additional support for an ionic ladder mechanism. If ladder switching is taking place and if $C_4H_3^+$ is formed from $C_4H_4^+$, the effect of delay should increase both $C_4H_3^+$ and $C_4H_4^+$ in the same manner since $C_4H_3^+$ would be formed from $C_4H_4^+$. The fact that exposure to the green laser decreases the $C_4H_4^+$ but increases the $C_4H_3^+$, and by increasing the delay increases the $C_4H_4^+$ but decreases the $C_4H_3^+$, suggests that the formation of both competes from the population of one electronic state of the parent ion.

The power dependence of the two components of $C_6H_5^+$ mass peak also suggests a competition mechanism rather than a sequential mechanism. It should be pointed out that one should not generalize this conclusion to other systems or even to other fragments of the 2,4-hexadiyne molecular ion. The study of the other fragments is now in progress and the complete work will be published soon.[7]

Acknowledgment. The authors thank E. Drollinger of E. G. and G. for making available to us the use of the boxcar integrator and signal processor. The financial support of NSF is greatly appreciated.

Registry No. 2,4-Hexadiyne, 2809-69-0.

(7) Gobeli, D. A.; El-Sayed, M. A. to be submitted to *J. Phys. Chem.*

Detection of Slow Motions in Oriented Lipid Multilayers by Two-Dimensional Electron-Spin-Echo Spectroscopy

Leela Kar, Glenn L. Millhauser, and Jack H. Freed*

Baker Laboratory of Chemistry, Cornell University, Ithaca, New York 14853 *(Received: May 2, 1984)*

The considerable potential of two-dimensional electron-spin-echo (2D-ESE) spectroscopy in the study of structure and dynamics in oriented media for spin probes undergoing slow molecular motions is demonstrated on a model membrane system doped with spin probe. A 90–τ–180 echo sequence is used to detect a variation of the homogeneous line width (T_2^{-1}) across the "echo-induced ESR spectrum". Simulations using recently developed methods are found to be very sensitive to parameters describing the rotational diffusion and the ordering potential. Rotational diffusion rates of the order of 10^4 s^{-1} are detected at temperatures below 0 °C, and a model of Brownian motion and a high ordering is found to characterize this smectic system consisting of low water content oriented multilayers of dipalmitoyl phosphatidylcholine (DPPC) doped with cholestane (CSL) spin probe. The great sensitivity of this 2D-ESE technique to a motional region inaccessible to cw studies is emphasized.

Introduction

ESR spectroscopy has proved to be of considerable value in studies of structure and dynamics in oriented fluids such as liquid crystals and oriented lipid–water systems.[1,2] This is especially true of the slow-motional regime, which, in principle, can supply considerable information.[1] However, as motions become slower, the line-shape analysis becomes very complex and, to some extent,

(1) "Spin Labeling, Theory and Applications", Berliner, L. J., Ed.; Academic Press: New York, 1976.
(2) Heminga, M. A. *Chem. Phys. Lipids* **1983**, *32*, 323.

0022-3654/84/2088-3951$01.50/0

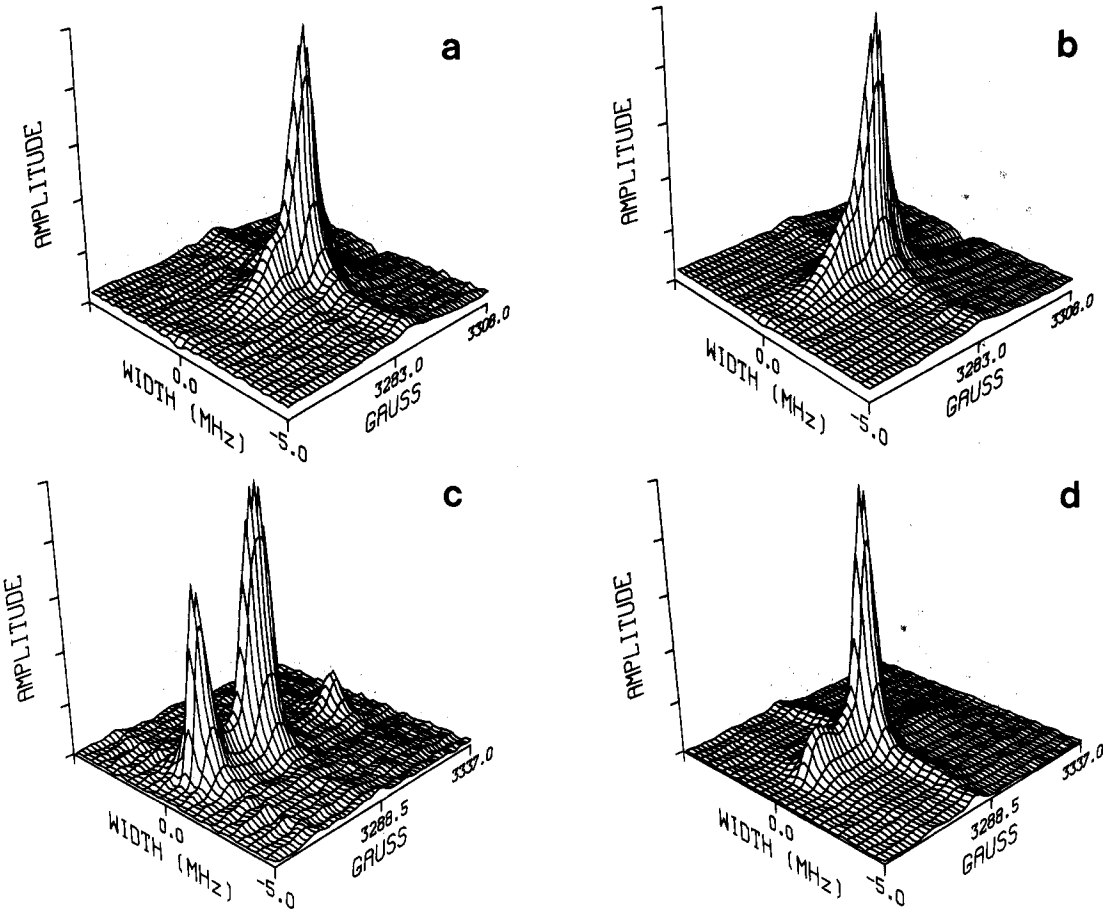

Figure 1. Experimental 2D-ESE spectra from oriented multilayers of low water content DPPC doped with CSL spin probe: (a) $\theta = 0°$, $T = 0$ °C; (b) $\theta = 0°$, $T = 20$ °C; (c) $\theta = 90°$, $T = 20$ °C; (d) $\theta = 45°$, $T = 20$ °C.

ambiguous. The resulting cw ESR spectra are largely inhomogeneously broadened, so the spectra tend to become model insensitive, and this obscures motional and structural information. These positive and negative features have been clearly illustrated in recent studies on thermotropic liquid crystals[3] and on oriented lipids.[4] Furthermore, as spectral simulations demonstrate, for rotational diffusion rates, $R \leq 10^5$ s^{-1}, the oriented cw spectra become insensitive to motional parameters, i.e., a cw ESR "rigid limit" is reached.

Millhauser and Freed (MF)[5] have very recently developed a technique of two-dimensional electron-spin-echo (2D-ESE) spectroscopy which is very sensitive for the study of slow molecular motions. In this technique an ESR spectrum is plotted along the x axis, while the *homogeneous* line shape is plotted along the y axis. Thus one obtains a simple map of the homogeneous T_2 as a function of field position in the spectrum. In a study on a small nitroxide probe in an isotropic viscous liquid, MF showed that, in general, T_2 will vary across the spectrum, and the features of this "T_2 plot" are not only very sensitive to motion in the region of $R \leq 10^6$–10^4 s^{-1} but also to the motional models used to describe molecular rotational reorientation.

In this Letter we wish to demonstrate the potential utility of this 2D-ESE technique in the study of oriented systems, in particular that it is "both an improvement on and a complement to"[5] the method of cw line-shape analysis for studying slow molecular motions. We report here our preliminary success with 2D-ESE spectroscopy on oriented lipid multilayers. Our objectives are twofold. We wish to (1) show how information regarding homogeneous line widths, and hence motional dynamics, may be extracted from these spectra; and also to (2) illustrate how the scope and sensitivity of the 2D-ESE technique may be used to special advantage in oriented media, where additional features of the dynamics and structure may be resolved, such as orienting potentials.

Experimental Section

The details regarding preparation of oriented low water content DPPC multilayers are reported elsewhere.[4] We basically follow the techniques of Powers and Pershan[6] and Asher and Pershan,[7] modified to suit our purposes. Anhydrous DPPC was obtained from Sigma and used without further purification. A uniform mixture of hydrated phospholipid (2–4% water by weight) and the spin-label CSL ([CSL]/[DPPC] = 1/200) is sealed between well-cleaned, surfactant-coated glass plates. Defect structures formed are thermally annealed by heating briefly to ~140 °C and then cooling in a controlled manner in order to maintain the homeotropic alignment produced at high temperatures. A Mettler FP52 automatic temperature control unit was used in conjunction with a Nikon polarizing microscope for this purpose. Sample dimensions are 0.7 cm × 3 cm × t where t, the multilayer thickness, varies from sample to sample (between 25 and 400 μm). Alignment of multilayers within each sample is checked both by polarizing microscopy[6,7] and cw ESR.[4] Although echoes are observable from a single sample in the cavity, five samples packed side by side (along their "thickness" direction) were used in the 2D-ESE experiments. The improvement in signal thus achieved is essential for 2D-ESE spectroscopy. The total multilayer thickness with five samples was ~700 μm. Standard ESE signals could be obtained over most of the temperature range of −150 to +140 °C.

(3) Meirovitch, E.; Freed, J. H. *J. Phys. Chem.*, in press and references therein.
(4) Kar, L.; Ney-Igner, E.; Freed, J. H., to be submitted for publication.
(5) Millhauser, G. L.; Freed, J. H. *J. Chem. Phys.* **1984**, *81*, 37.
(6) Powers, L.; Pershan, P. S. *Biophys. J.* **1977**, *20*, 137.
(7) Asher, S. A.; Pershan, P. S. *Biophys. J.* **1979**, *27*, 393.

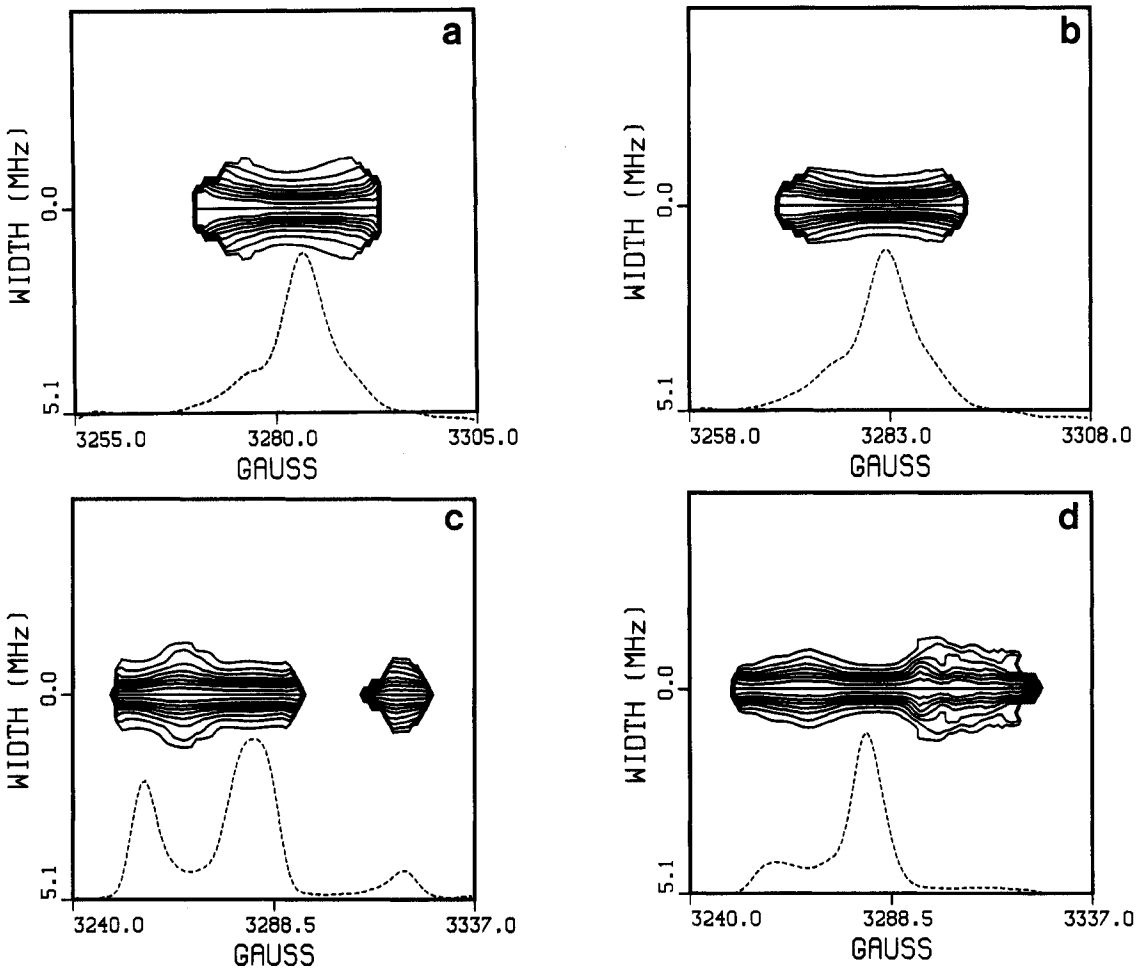

Figure 2. Experimental 2D-ESE normalized contours corresponding to the spectra of Figure 1 (a, b, c, d as in Figure 1). Each successive contour line represents a 10% change relative to the normalized maximum. Shown at the bottom of each plot is the 0-MHz spectrum. We have deleted the low amplitude contours, since their signal to noise is low. The vertical lines at each end closing the contours are artifacts of the plotting routines and should be ignored.

The ESE spectrometer used has been described elsewhere.[8] The modifications and interfacing required for 2D-ESE spectroscopy is discussed by MF. Basically, the echo amplitude resulting from a 90–τ–180 pulse sequence is monitored by sweeping the magnetic field in a synchronous fashion across the nitroxide (CSL) spectrum. Typically 50–60 scans were performed at various τ values, each scan consisting of 500 data points. The 90° pulse width used was 80 ns which corresponds to a weak enough microwave field H_1 that the "echo-induced ESR" signal is undistorted. The data are then Fourier transformed as a function of τ for each field value. The 2D-ESE experiment was performed for three different angles (θ = 0°, 45°, 90°) between the common normal to the set of five sample sandwiches and the external dc magnetic field. For CSL in low water content DPPC multilayers, this angle, θ, coincides with the angle between the director and the external field, since the regions of the hydrocarbon chains of DPPC probed by CSL remain normal to the bilayer plane at the temperatures of the experiment.[4]

MF show that the 2D-ESE slow-motional signal may be written as

$$S(\omega,\omega') \propto \sum_j a_j^2 \left(\frac{T_{2j}}{1 + \omega^2 T_{2j}^2} \right) (e^{-2\tau_d/T_{2j}}) \exp[-(\omega' - \omega_j)^2/\Delta^2] \quad (1)$$

That is, the 2D-ESE spectrum is a sum over "dynamic spin packets" with natural widths T_{2j}^{-1}, and resonance frequency ω_j, and relative weight a_j^2. [These are the normal-mode solutions from the stochastic Liouville equation.[9]] An ESR-like absorption spectrum is obtained along $\omega' = \gamma_e H_0$ and is inhomogeneously broadened with an assumed Gaussian width, Δ. Along the ω axis one observes a blend of Lorentzian line shapes from the various "dynamic spin packets". In general, we find that while T_2 varies across the spectrum, the observed 2D-ESE line shapes at each position ω' is a simple Lorentzian in ω. The dead time, τ_d, of our ESE spectrometer is currently about 150–200 ns. This was accounted for in both the data processing and the theoretical analysis. In our analysis we found it important to add to the T_{2j}^{-1} an orientation-independent and virtually temperature-independent contribution, $(T_2^{ss})^{-1}$, that was measured at lower temperatures ($T \leq -50$ °C) and was ascribed to solid-state spectral diffusion processes.

Results and Discussion

Figure 1a–d shows the spectra (after Fourier filtering and Fourier transformation)[5] from a 90–τ–180 pulse sequence. Although not yet useful for extracting line-shape information in this form, the 2D surfaces illustrate the great spectral variations obtainable from a sample with both microscopic and macroscopic order (compare parts b, c, and d of Figure 1 for θ = 0°, 90°, and 45°, respectively, at temperature, T = 20 °C).

Information regarding molecular structure and dynamics is more readily obtained when the 2D surfaces are reduced to normalized contour plots. This representation is developed by dividing every slice of the spectrum along the "width" (or ω) axis by its corresponding amplitude at 0 MHz and then generating

(8) Stillman, A. E.; Schwartz, L. J.; Freed, J. H. *J. Chem. Phys.* **1980**, *73*, 3502.

(9) (a) Moro, G.; Freed, J. H. *J. Phys. Chem.* **1980**, *84*, 2837. (b) Moro, G.; Freed, J. H. *J. Chem. Phys.* **1981**, *74*, 3757.

contour lines at every 10% change in height. The resulting map reveals the homogeneous line shape as a function of field location unaffected by differences in signal height. We also provide the unnormalized slice along the field direction at 0 MHz to show how the contours relate to the ESR spectrum. Figure 2a–d shows the normalized contour plots corresponding to the 2D surfaces shown in Figure 1.

The way in which the contours vary across the spectrum can be understood qualitatively.[5] The regions of the spectrum with maxima in height correspond to those probe molecules that have a principal axis (of the magnetic tensor) aligned parallel to the dc magnetic field. For these molecules, the orientation-dependent part of the spin Hamiltonian is only weakly affected by small angle (i.e., Brownian) reorientations. Phase memory relaxation, which results from random modulation of the spin Hamiltonian, is thus suppressed in these spectral regions and the contours show a narrowing. In this simple picture the ordering potential primarily restricts the range of angles the molecule can sample.

One may observe that our theoretical treatment is successful in simultating these effects for an ordered system. Figure 3a–c shows simulated contours corresponding to the experimental results in part a, b, and c of Figure 2. In these simulations we have used the **A** and **g** tensors for CSL as determined from rigid-limit cw ESR spectra from these samples at $T \leq -75$ °C.[4] An axially symmetric ordering potential was used to describe the potential experienced by the probe molecules. We explored the effects of varying the ordering potential on the predicted contours (compare Figure 3a with Figure 4c and d), but our best fits correspond to the ordering obtained from the cw line-shape analysis at the "rigid limit".[4]

A Brownian model for molecular motion appears to predict the appropriate contour shapes obtained at both $T = 0$ °C and $T = -20$ °C (compare Figure 2a, and b, with Figure 3, a and b). The effect of a decrease in temperature is appropriately simulated by a corresponding decrease in the rotational diffusion rate of the probe molecule (from $R = 10^4$ s^{-1} to $R = 8 \times 10^3$ s^{-1}). We considered motional anisotropy for the Brownian diffusion model and found that simulated contours agree well with experimental results only for small values of N ($=R_\parallel/R_\perp$).[1] We illustrate the effects of introducing motional anisotropy in two ways: (1) $R_\perp$ is kept unchanged and $R_\parallel$ is varied; (2) both $R_\perp$ and $R_\parallel$ are varied, keeping the geometric mean ($(R_\perp R_\parallel)^{1/2}$) unchanged. Comparison of Figure 3b with 4a shows that changing the value of N from 1 to 5 by method (1) has a significant effect on the 2D contours, in spite of the fact that the $\theta = 0°$ orientation is less sensitive to changes in $R_\parallel$ than in $R_\perp$. When the geometric mean is kept constant, the effect of varying N on the 2D contours is more subtle (compare Figure 3, a and b, with 4b). Although the differences corresponding to this small range of N are not large, both the 2D contour and the 0-MHz slice for $N = 1$ fit the experiment better than $N = 5$. For a long, rigid probe molecule like CSL, the rate of rotation around the parallel axis ($R_\parallel$) is expected to be faster than that around the perpendicular axis ($R_\perp$). From cw ESR line shape analysis values between 5 and 1000 for CSL at various temperatures have been predicted in thermotropic smectic phases.[3,10] For the lyotropic system reported here (i.e., CSL in DPPC–H_2O), the cw ESR line-shape analysis has led to predictions of N of 25 to 100 for $T \geq 23$ °C.[4] However, the sensitivity of the simulations to N differs vastly in these techniques.

For the slow-motional (low T) region relevant here, cw line-shape analysis is rather insensitive to motional parameters $R_\perp$, $R_\parallel$ and hence N. Changes by more than an order of magnitude are required before significant effects are observed in the predicted spectra. 2D-ESE, on the other hand, is seen to be sensitive to both the rate (compare Figure 3, a and b) and the anisotropy in the rotational diffusion tensor (compare Figure 3, a and b, with 4, a and b). For a Brownian model, an isotropic rotational diffusion tensor appears to fit the experimental results best. However, we would like to point out that for these preliminary studies we have considered only the simplest of molecular models for our simulations. More complex models of rotational diffusion (for example, considering a tilt angle between the principal axes of molecular diffusion and the magnetic tensor frame), and microscopic ordering may be required to simulate the physical situation more accurately. Although our computer programs are fully capable of handling such complex models,[9] we reserve these for more detailed studies in the future. That our molecular model is a reasonable first approximation is shown by the closeness of fit between the experimental and simulated contour plot corresponding to $\theta = 90°$ (compare Figures 2c and 3c).

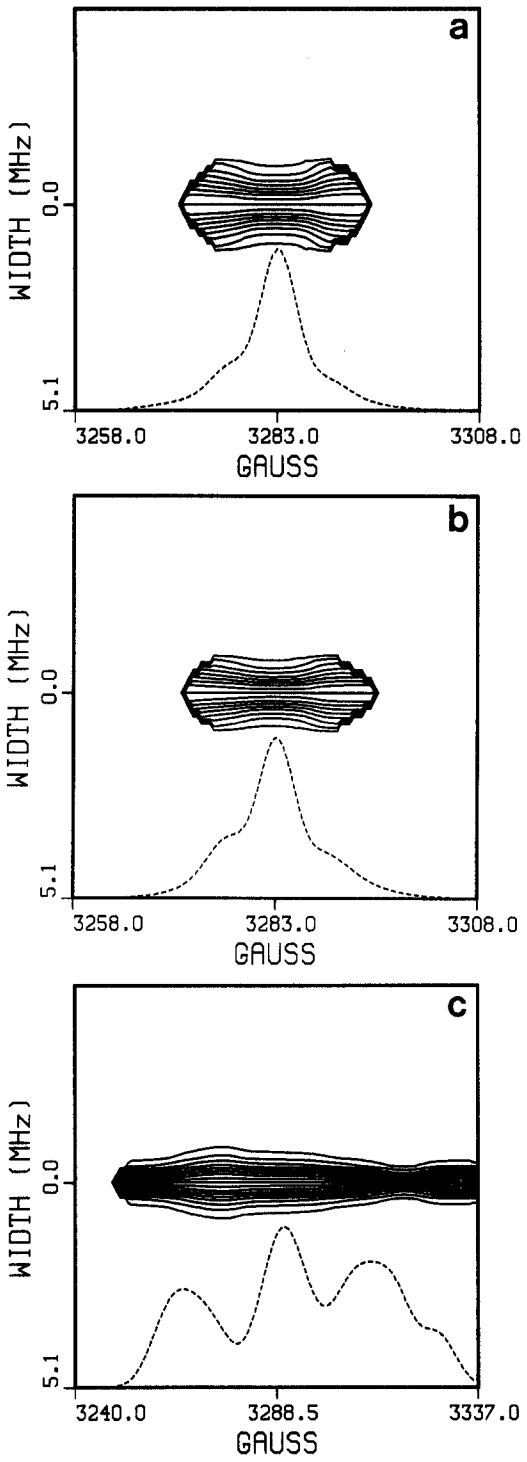

Figure 3. Simulations of 2D contours to compare with experiment: (a) $\theta = 0°$, $R_\parallel = R_\perp = 1 \times 10^4$ s^{-1}, $\lambda_0^2 = 8.0$ ($\langle D^2_{00} \rangle = 0.87$); (b) $\theta = 0°$, $R_\parallel = R_\perp = 0.8 \times 10^4$ s^{-1}, $\lambda_0^2 = 8.0$; (c) $\theta = 90°$, other parameters as in (b). Also, $T_2^{ss} = 0.7$ μs, $\tau_d = 0.2$ μs, and $\Delta = 3.2$ G in a and b, but 6.0 G in c. Compare parts a, b, and c to part a, b, and c of Figure 2, respectively.

(10) Meirovitch, E.; Freed, J. H. *J. Phys. Chem.* **1980**, *84*, 2459.

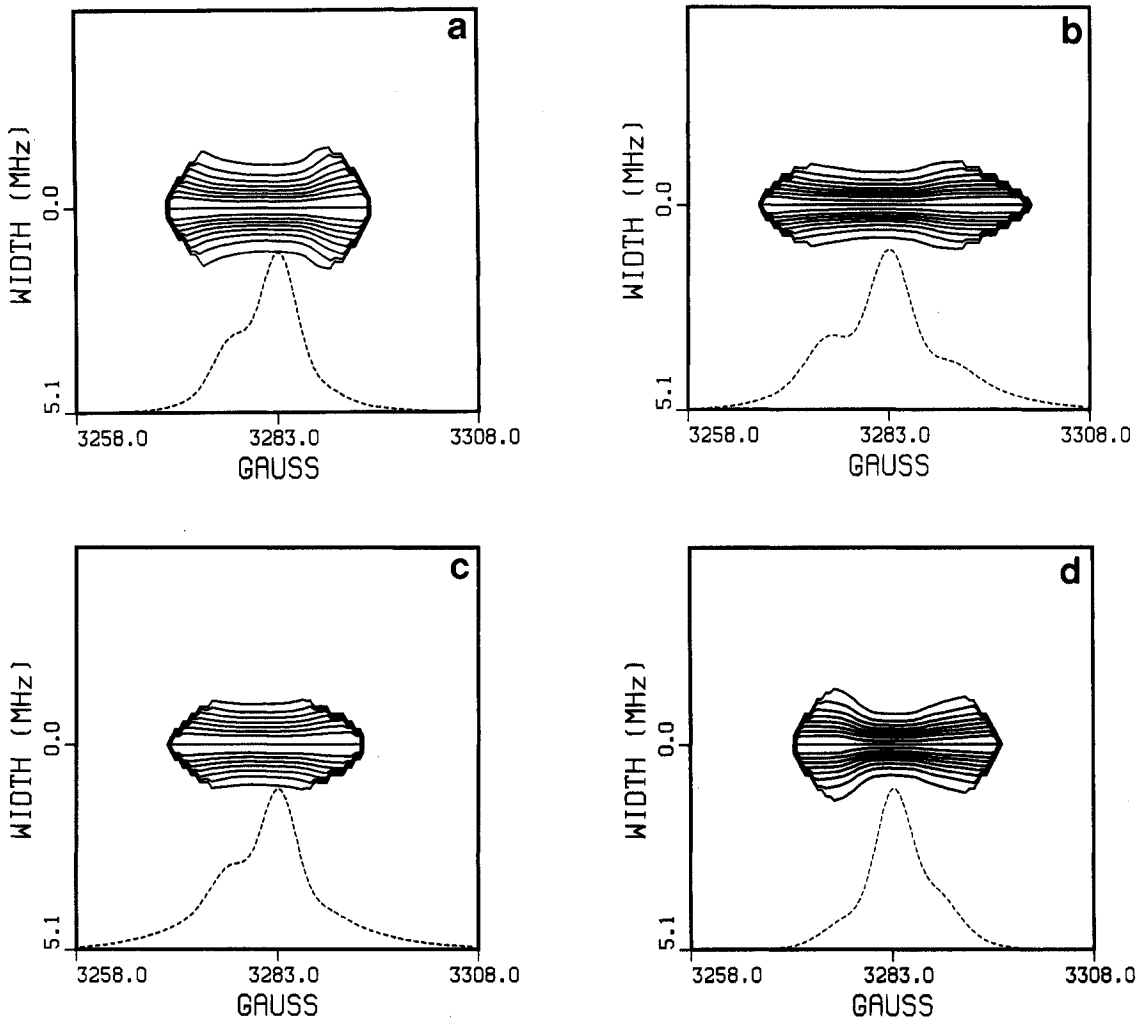

Figure 4. Simulations of 2D contours for $\theta = 0°$ to illustrate sensitivity to motion and ordering: (a) $R_\parallel = 4 \times 10^4\ s^{-1}$, $R_\parallel = 0.8 \times 10^4\ s^{-1}$, or $N = 5$, $\lambda_0^2 = 8.0$; (b) $R_\parallel = 2 \times 10^4\ s^{-1}$, $R_\perp = 0.5 \times 10^4\ s^{-1}$, or $N = 4$, $\lambda_0^2 = 8.0$; (c) $R_\parallel = R_\perp = 1 \times 10^4\ s^{-1}$, $\lambda_0^2 = 4.0$ ($\langle D_{00}^2 \rangle = 0.71$); (d) $R_\parallel = R_\perp = 1 \times 10^4\ s^{-1}$, $\lambda_0^2 = 12.0$ ($\langle D_{00}^2 \rangle = 0.91$). Other parameters are as in Figure 3.

An alternative explanation for similar values of $R_\parallel$ and $R_\perp$ could be that there is some "molecular flexing" or internal rotation involved, and at these low temperatures the rotational diffusion rate is of the same order of magnitude as such a mode of internal motion.

A more accurate estimation of N could be obtained from detailed simulations as a function of tilt-angle θ.[3,4] However, it must be noted here that for the present case of very slow motion and high ordering the theoretical simulation of spectra represents a considerable challenge. In particular, the size of the stochastic Liouville matrix and the number of nonzero matrix elements becomes enormous. Moreover, both increase greatly for $\theta \neq 0°$, since the cylindrical symmetry of the problem in the laboratory frame is lost. We did achieve convergent 2D-ESE spectral simulations for the $\theta = 0°$ cases, but those we obtained for $\theta = 90°$ were not, even though they involved over 8000 basis vectors. This challenge arises precisely because the 2D-ESE spectra are sensitive to such slow motions, and we plan to consider these matters in future work. (Since the $\theta = 45°$ case has even less symmetry than that for $\theta = 90°$, we did not attempt to simulate the 45° spectrum.) The nonconvergence is evident in the peculiar line shape of the 0-MHz slice shown below the 2D contours in Figure 3c. However, simulations show that the 2D-ESE contours tend to reach convergence faster than the cw line shape. We have therefore used the set of eigenvectors and eigenvalues of this nonconverged problem to generate the 2D contours in Figure 3c.

Inclusion of the T_2^{ss} (estimated to be 700 ns) has two effects on the appearance of the calculated contours. (1) The predicted widths along the ω axis are increased, and (2) the variation in T_2 across the spectrum is reduced, as the effects of dynamic spin packets with $T_{2j} > T_2^{ss}$ are suppressed. On the other hand a finite τ_d reduces the amplitudes of the fast decaying "dynamic spin packets" with $T_{2j} < \tau_d$ (cf. eq 1) such that contour regions of broad width become more narrow. This also reduces the variation in T_2 across the spectrum. Thus both τ_d and T_2^{ss} act to even out variations in the contours, such that only those T_{2j} obeying $\tau_d < T_{2j} < T_2^{ss}$ are important. This also means that T_2^{ss} prevents one from studying slower motions with $R < 10^4\ s^{-1}$, while $\tau_d = 150$–200 ns makes it difficult, with existing signal-to-noise, to obtain 2D-ESE spectra from faster motions with phase memory times $T_{2j} < 150$ ns corresponding to $R > 10^6\ s^{-1}$. Thus efforts to reduce τ_d and to suppress T_2^{ss} by other pulse sequences would be desirable and are currently under way in our laboratory.

Despite these limitations we believe that the application of the technique to model membrane systems is nicely illustrated by the experiments described here. We now wish to emphasize the sensitivity of this technique to structural and dynamic features. In particular, one finds that the predicted contours change significantly even from small changes in both motional and ordering parameters, and we illustrate this with a few examples in Figures 3 and 4. In these cases, which relate to the experimental results of Figures 1 and 2, the inhomogeneous width Δ is 3.2 G, yet the entire 2D-ESE contour is mapped out for $\omega/\gamma_e \sim 1.5$ G corresponding to *homogeneous* widths of the order of 0.1 G. This is an important source of the sensitivity of the 2D-ESE method. Note also, that the $\omega = 0$ MHz slices also show sensitivity beyond

ordinary cw spectra. We attribute this to their direct dependence on the $T_{2,j}$ according to eq 1.

We expect that as 2D-ESE techniques are further developed, they will provide a very useful method to enable detailed studies of structure and dynamics in oriented media.

Acknowledgment. This work was supported by NIH Grant GM 25862, NSF Grants DMR 81-02047 and CHE 8319826, and by the Cornell Materials Science Center.

Registry No. DPPC, 2644-64-6.

FEATURE ARTICLE

Chemical Dynamics Studied by Emission Spectroscopy of Dissociating Molecules

Dan Imre, James L. Kinsey,* Amitabha Sinha, and John Krenos†

Department of Chemistry, Massachusetts Institute of Technology, Cambridge, Massachusetts 02139
(Received: November 29, 1983)

The use of absorption and emission spectroscopy of photodissociating molecules is discussed as a means of probing details of dissociation dynamics in extremely short-lived transient species. The study of photodissociation processes has special advantages which derive from the special ability to create well-defined initial conditions and from the simplicity of interpretation of experimental results. Casting the absorption and emission processes in a time-dependent formalism developed by Heller and co-workers enables intuitive connections to be made between spectroscopic features and the underlying dynamics. The absorption spectrum of photodissociating molecules primarily contains information about very short-time dynamics, whereas the emission spectrum reveals more details and encompasses intermediate times as well. Information about both the excited-state and the ground-state potential surfaces is contained in the emission spectrum. Intensities of fundamentals, overtones, and combinations can be used to infer properties of the upper-state surface (such as forces and their gradients). The observed energies and band contours of the same features yield characteristics of the ground-state surface. Experimental results on methyl iodide and ozone are used to illustrate how emission spectra can be used to study reaction dynamics.

I. Introduction

In every elementary chemical reaction the molecular system passes through a continuously evolving intermediate species that is neither reactant nor product but the former in the process of turning into the latter. No great insight is required to appreciate that the more we learn about these intermediate species the better we will understand the transformation. Theoretical techniques for treating dynamics of small polyatomics have advanced to the point where fairly accurate predictions can be made.[1-3] What is still lacking is experimental data that can be used to supply information for these calculations and to test them. As experimentalists our goal is to devise a scheme which will enable a direct and "meaningful" observation of the reaction intermediate. Here the word "meaningful" refers to the ability to easily extract information which can be utilized as initial estimates in dynamical calculations. The hope, of course, is that by combining a few detailed experimental results with complete calculations, we can get a global picture of both intra- and intermolecular dynamics.

In a recent elegant feature article in this journal, Foth et al.[4] surveyed a variety of methods for studying photon emission from molecules and reaction intermediates in the process of falling apart. The purpose of our report is an elaboration, from a different point of view, of some of the aspects mentioned in the Foth paper, i.e., the absorption and emission spectroscopy of photodissociating molecules. Our approach, which rests on a time-dependent formulation of photon absorption and emission developed by Heller and co-workers,[5] will emphasize the power in the inherent equivalence of time and frequency information in such experiments. We will use our results from methyl iodide and ozone UV photodissociation studies to illustrate how absorption and emission spectroscopy can be used to study reaction dynamics. We will show that even at a qualitative level very instructive information can be extracted. These two molecules were selected because they exhibit quite different nuclear motion on their path to unimolecular dissociation.

We will start by discussing some of the general considerations to be taken into account when selecting a dynamical process for study. In section III we point out the advantages offered by the relative simplicity of photodissociating systems as compared to bimolecular reactions. Section IV describes the experiental approach which we have adopted for investigating photodissociation reactions. Here, we also make the connection between the spectroscopic data obtained experimentally and the dynamics in question. Section V discusses our experimental results for CH_3I and O_3.

II. Experimental Design Considerations

The detailed study of nuclear motion during a reactive collision is an experimental challenge since the reaction time is typically less than 1 ps. Consequently, understanding the fine details would require knowledge of the dynamics on a femtosecond time scale. Or, to put it in a different perspective, during the time of interest the molecular system experiences structural changes on a scale of a few few angstroms. Knowledge of the time evolving structure with subangstrom resolution is equivalent to knowing the dynamics on roughly a femtosecond time scale. In order to yield the needed

† Visiting Associate Professor 1982-83. Permanent address: Department of Chemistry, Rutgers University, New Brunswick, NJ 08903.

(1) S. Y. Lee and E. J. Heller, *J. Chem. Phys.*, **76**, 3035 (1982).
(2) M. Shapiro and R. Bersohn, *J. Chem. Phys.*, **73**, 3810 (1980).
(3) D. Truhlar, Ed., "Potential Energy Surface and Dynamic Calculations", Plenum Press, New York, 1981.
(4) H. J. Foth, J. C. Polanyi, and H. H. Telle, *J. Phys. Chem.*, **86**, 5027 (1982).
(5) (a) E. J. Heller, *Acc. Chem. Res.*, **14**, 368 (1981); (b) E. J. Heller, R. Sundberg, and D. Tannor, *J. Phys. Chem.*, **86**, 1822 (1982); (c) E. J. Heller, *J. Chem. Phys.*, **68**, 2066 (1978); (d) S. Y. Lee and E. J. Heller, *ibid.*, **71**, 4777 (1979).

0022-3654/84/2088-3956$01.50/0